Nuclear Instruments and Methods in Physics Research A 829 (2016) 159–162

Contents lists available at ScienceDirect

Nuclear Instruments and Methods in Physics Research A

journal homepage: www.elsevier.com/locate/nima

Investigation of ion acceleration mechanism through laser-matter interaction in femtosecond domain

C. Altana [a,b,*], A. Muoio [a,c], G. Lanzalone [a,d], S. Tudisco [a], F. Brandi [e,f], G.A.P. Cirrone [a], G. Cristoforetti [e], A. Fazzi [g], P. Ferrara [e], L. Fulgentini [e], D. Giove [g], P. Koester [e], L. Labate [e,h], D. Mascali [a], D. Palla [e,h,i], F. Schillaci [a], L.A. Gizzi [e,h]

[a] Istituto Nazionale di Fisica Nucleare, Laboratori Nazionali del Sud, Via S. Sofia 62, 95123 Catania, Italy
[b] Dipartimento di Fisica e Astronomia, Università degli Studi di Catania, Via S. Sofia 64, 95123 Catania, Italy
[c] Dipartimento di Fisica e Scienze della Terra, Università degli Studi di Messina, Viale F.S. D'Alcontres 31, 98166 Messina, Italy
[d] Università degli Studi di Enna "Kore", Via delle Olimpiadi, 94100 Enna, Italy
[e] CNR, Intense Laser Irradiation Laboratory, Via G. Moruzzi 1, 56124 Pisa, Italy
[f] Istituto Italiano di Tecnologia, Via Morego 30, 16163 Genova, Italy
[g] Energy Department, Polytechnic of Milan and INFN, Milan, Italy
[h] Istituto Nazionale di Fisica Nucleare, Sezione di Pisa, Largo B. Pontecorvo 3, 56127 Pisa, Italy
[i] Dipartimento di Fisica, Università di Pisa, Largo B. Pontecorvo 3, 56127 Pisa, Italy

ARTICLE INFO

Available online 11 February 2016

Keywords:
Acceleration measurement
Ions spectrometer
Ion energy distribution

ABSTRACT

An experimental campaign aiming to investigate the ion acceleration mechanisms through laser-matter interaction in the femtosecond domain has been carried out at the ILIL facility at a laser intensity of up to 2×10^{19} W/cm^2. A Thomson Parabola Spectrometer was used to identify different ion species and measure the energy spectra and the corresponding temperature parameters. We discuss the dependence of the protons spectra upon the structural characteristics of the targets (thickness and atomic mass) and the role of surface versus target bulk during acceleration process.

1. Introduction

Recent developments in laser technology allow high-density and high-temperature plasmas to be generated by means of laser-matter interaction, thereby producing and accelerating ion beams in the tens of MeV energy range [1,2].

Potential applications in different fields are being considered including proton therapy, fast ignition of inertial confinement fusion, neutron generation and study of nuclear physics phenomena. It is already understood that the ion production in laser-produced plasma is related to hot electrons. The commonly recognized effect responsible for ion acceleration is charge separation in plasma due to high energy electrons driven by the ultra-intense laser-target interaction. Protons and heavier ions can be accelerated, following the initial electron acceleration, to tens MeV per nucleon via a well-known mechanism, namely target normal sheath acceleration (TNSA) [3–5]. Fast electrons are accelerated by an intense laser pulse ($I \geq 10^{19}$ W/cm^2) at the surface of a thin foil in the forward direction. Electrons penetrate the foil, escape at the rear side of the target inducing a strong longitudinal electric field which ionizes atoms in the surface layer and accelerates them in the target normal direction. Typically, this field accelerates simultaneously several ion species, originated partly from the bulk target material, but predominantly from the hydrocarbon contaminant layers present on both sides of the target foils. Therefore spectrometers with adequate charged species discrimination capability allow the energy spectra of individual ion species to be detected.

Nowadays there are open questions about the dependence on target thickness and resistivity [6], and surface or volume contribution. In this context, we carried out a systematic experimental investigation to identify the role of target properties in TNSA, with special attention to target thickness and dielectric properties. Here we present some preliminary experimental findings obtained in this investigation including results showing contribution of bulk ions to the acceleration process and dependence of the ion temperature on the target parameters.

We used a full range of ion detector, optical, X-ray [7] and fast electrons [8] diagnostics to investigate laser-plasma interaction, fast electron transport and ion acceleration. In this paper we focus

* Corresponding author at: Istituto Nazionale di Fisica Nucleare, Laboratori Nazionali del Sud, Via S. Sofia 62, 95123 Catania, Italy.
E-mail address: altana@lns.infn.it (C. Altana).

http://dx.doi.org/10.1016/j.nima.2016.02.016
0168-9002/

on the results of ion detection obtained by using a Thomson Parabola Spectrometer (TPS).

In the TPS ions with different charge-to-mass ratios are separated into distinct parabolas. This allows information for each ion species to be extracted when several ions are generated simultaneously in a given solid angle. The working principle, widely described in literature [9–12], is based on parallel electric and magnetic fields acting on a highly collimated ion beam propagating orthogonally to the fields. The Lorentz force splits the different ion species according to their charge-to-mass ratio and energy. This yields a series of parabolic traces on the detector, each of them corresponding to well determined ion species having different charge to mass ratio.

2. Experimental set-up

The experiments have been performed at the Intense Laser Irradiation Laboratory (ILIL) in Pisa where a Ti:Sapphire laser system is operating, which delivers 40 fs – 800 nm pulses with energy on target up to 450 mJ. The ILIL laser pulse exhibits an ASE contrast greater than 10^{10} and a ps contrast of 10^5 at 1 ps before the peak pulse. The beam is focused on the target at an angle of incidence of 15° using an off-axis parabolic mirror; the corresponding maximum intensity on target was up to 2×10^{19} W/cm^2. The target was mounted on a three-axis translation stage system at the center of a 640 mm diameter interaction chamber. TPS was placed normal to the target rear side, housed in a separate vacuum chamber, operating at a pressure of 10^{-6} Torr, and differentially pumped with respect to the main target chamber. Details of TPS are given elsewhere [13–15]. The ions position is detected using an imaging system consisting of a micro-channel plate coupled to a phosphor screen, 75 mm in diameter (MCP-PH), and an EMCCD camera. Fig. 1 shows a sketch of the experimental setup.

Targets consisting of different materials (metal and plastic) and thickness were used, with a thickness ranging from 2 μm to 12 μm.

3. Data analysis and results

The spectrogram images of EMCCD contain a bright halo, which constitutes the origin of the parabolic ion traces, due to x-radiation and neutral particles propagating straight through the electromagnetic field, and parabolic traces associated to protons and heavier ions outgoing from the bright region, as shown in Fig. 2.

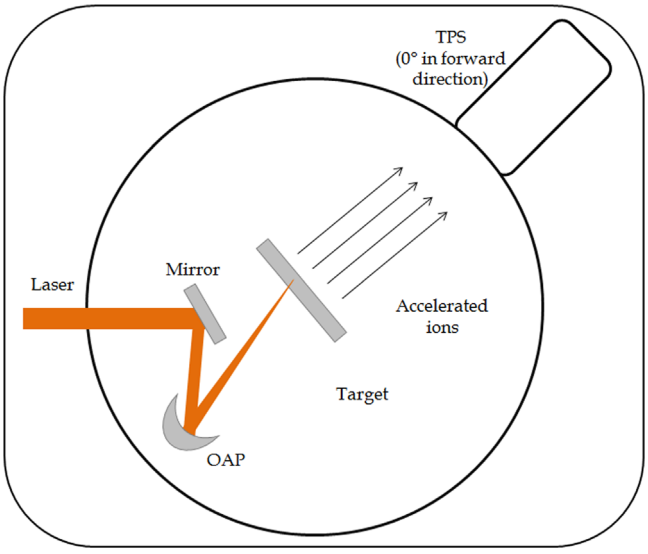

Fig. 1. Sketch of the experimental set-up.

Procedure to analyze spectrograms consists of different steps. First step is to crop the image in the parabolas vertex and to overlap the theoretical parabolas to the spectrogram. Then the energy spectra of different ion species and charge states are reconstructed by cutting out the events associated to the parabolas and by using one of the equations reported in Ref. [16] related to the magnetic or electric deflections. Fig. 3 shows an example of such reconstruction for protons emitted during the irradiation of a CD_2 target. The reconstruction by using both the equation related to the magnetic and electric deflections is an important cross-check to verify all the

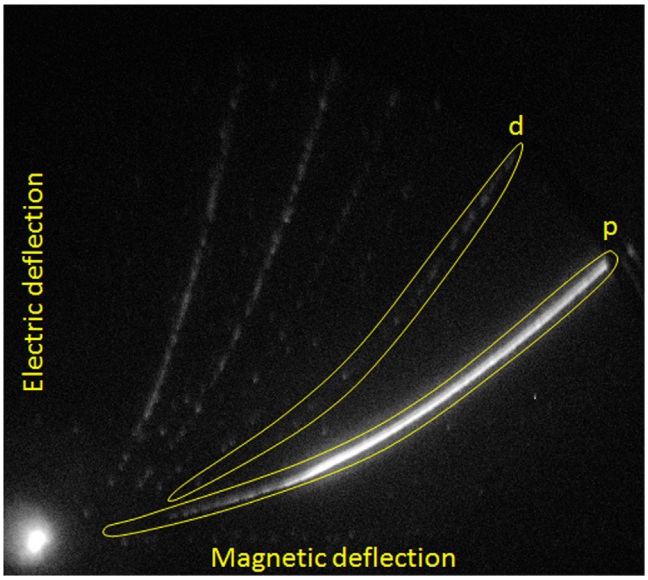

Fig. 2. TPS spectrogram from CD_2 target: protons, deuterons and carbons with different charge states are detected. The yellow curves represent the cuts used in order to reconstruct the spectra for protons and deuterons. (For interpretation of the references to color in this figure legend, the reader is referred to the web version of this article.)

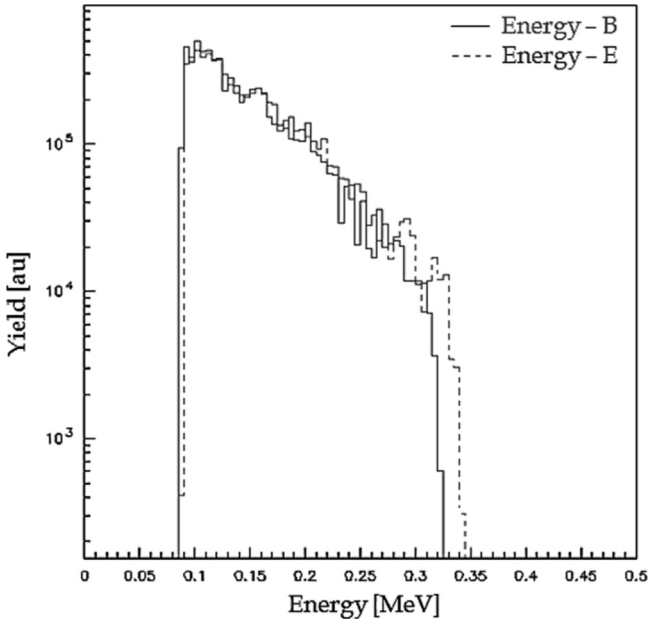

Fig. 3. A sample proton spectrum reconstructed by means of magnetic (solid line) and electric (dotted line) deflections. The trend of the MCP brightness is shown as a function of the ion's kinetic energy. The spectra are well overlapped.

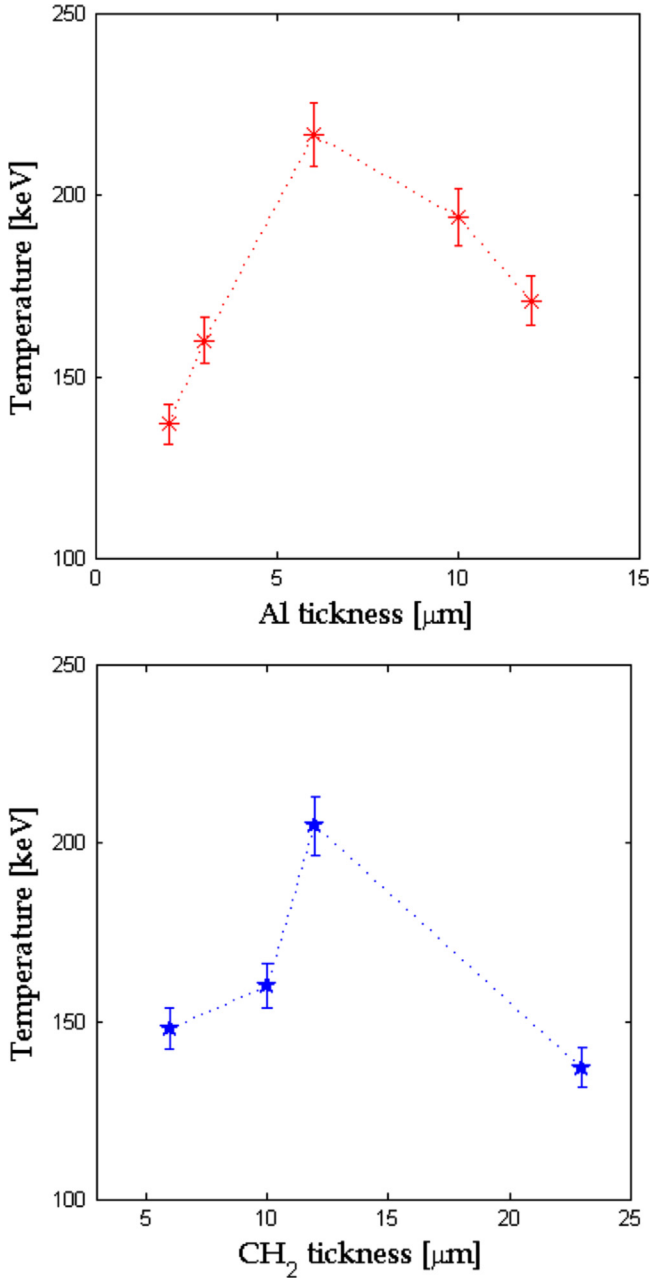

Fig. 4. Proton temperature obtained as function of target thickness for Al (top) and CH_2 (bottom).

TPS alignments; in such condition we checked the profiles by using both the methods, i.e. by using independently the energy reconstruction by the electric or magnetic deflection. When the spectra were observed to assume the same shape this was argued as a condition of perfect working condition and alignment.

The obtained energy spectra show an exponential like trend, which has been fitted in first approximation with a Boltzmann-like distribution; a temperature parameter has been extracted and related to the shoot conditions.

3.1. Target thickness dependence

Temperature parameters of protons from aluminum (metallic) and CH_2 (plastic) as function of target thickness are shown in Fig. 4.

Table 1
Protons and deuterons temperature obtained from CD_2 and CD_2+Al target.

Temperature [KeV]	CD_2	CD_2+Al
Protons	**102 ± 5**	**152 ± 8**
Deuterons	**53 ± 3**	**17.8 ± 0.9**

From these plots it is possible to observe that the maximum protons temperature of 217 keV is found for the 6 μm thick Al target, while a temperature of 205 keV was found for the 12 μm CH_2 target. In both cases the maximum temperature increases up to an optimum thickness and then falls down with increasing target thickness.

3.2. Surface vs. bulk dependence

In order to understand if accelerated ions are due to surface contamination or bulk ions, we compared data from 10 μm CH_2 targets with 10 μm CD_2 targets as previously studied in [17,18]. In fact, in the case of CH_2 targets accelerated protons may originate from the target surface as well as from the bulk. In contrast, in the case of CD_2, protons will predominantly come from the surface, while deuterons may originate only from the bulk.

In a previous work [17] we showed the result of a focal scan in which protons and deuterons spectra were measured for different positions of the target foil relative to the laser focal spot. Protons and deuterons temperatures were found to exhibit opposite trends, with protons showing a maximum temperature in the best focus position, while deuterons showing a minimum temperature.

Following this indication, we performed further investigation using CD_2 target coated with an Al layer of about 1 μm on the laser irradiated side.

Table 1 shows the results of Al coated and uncoated CD_2 targets. As can be noticed, CD_2+Al target show a higher proton temperature while CD_2 target exhibit a lower deuterons temperature.

The effect of Al layer on the proton temperature can be justified by the more efficient generation of hot electrons in Al than in plastic due to the higher electron density in the interaction region which can also compensate the increase of target thickness due to the 1 μm Al layer. Concerning the lower deuteron temperature observed, the explanation requires further investigation in view of the fact that the deuterons originate from the bulk of the target and, therefore, the acceleration process is not fully understood at this stage. We can speculate that the presence of the additional Al layer may reduce the effect of direct laser radiation of the CD_2 substrate, thus yielding lower deuteron temperature. These aspects are currently under investigation and will be discussed in a future publication. However the results need further theoretical and experimental investigation to be fully understood.

3.3. Atomic or molecular mass dependence

Finally, we show in Fig. 5. the protons temperature dependence as function of the atomic or molecular mass by using all the data from the irradiation of CD_2, Al and 5 μm thick titanium targets.

A linear dependence on target mass is clearly visible suggesting in first approximation that targets consisting of heavier materials will lead to an increases of the proton temperature and, consequently, maximum proton energy.

Of course such preliminary results need further experimental and theoretical work in order to understand in such contest the effects for example of the target thickness, the electron transport and the influence of the boundary experimental conditions (e.g. pre-pulse effects [19]).

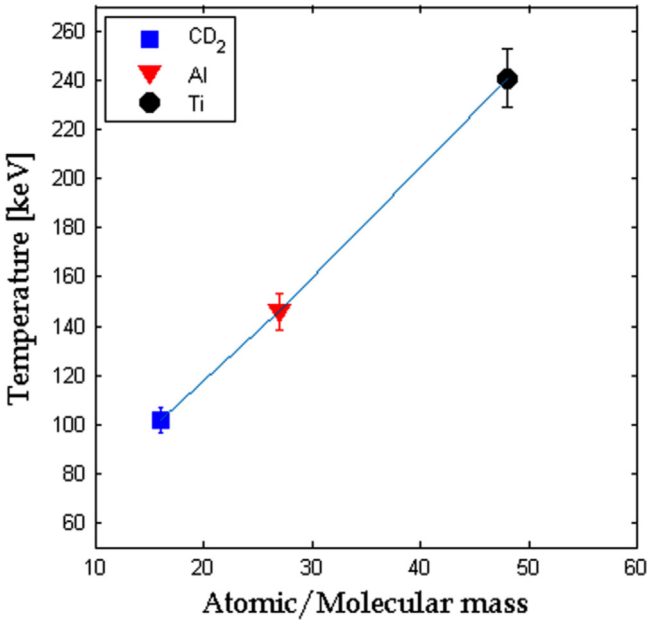

Fig. 5. Linear trend of protons temperature for different target as function of atomic or molecular mass.

4. Conclusion

Ion acceleration mechanism in TNSA regime was investigated by using a Thomson Parabola Spectrometer. Protons spectra were obtained for different target materials and thicknesses. The higher proton temperature was found for 6 μm Al and 12 μm CH_2.

Surface versus volume contributions to the ion acceleration have been identified by using a unique target configuration consisting of a thin CD_2 foil and comparing it to CH_2 targets with the same thickness. Preliminary results show that protons and deuterons temperatures show opposite trend, suggesting different acceleration process and a complex interplay between surface and volume acceleration. Moreover, the use of a thin Al layer was found to be effective in increasing the proton temperature. Finally, a linear dependence from atomic or molecular mass of the target was obtained with highest temperature found for titanium target.

Further studies of heavy target material and thickness are in progress.

Acknowledgments

We acknowledge financial contribution from the ELIMED and G_RESIST projects of the INFN CN5 and from the ELI-Italy Network funded by the MIUR. This work is partially supported by the MIUR-PRIN 2012 (Contract No. PRIN2012AY5LEL).

References

[1] E.L. Clark, K. Krushelnick, M. Zepf, F.N. Beg, M. Tatarakis, A. Machacek, M.I. K. Santala, I. Watts, P.A. Norreys, A.E. Dangot, Physical Review Letters 85 (2000) 1654.
[2] M. Hegelich, S. Karsch, G. Pretzler, D. Habs, K. Witte, W. Guenther, M. Allen, A. Blazevic, J. Fuchs, J.C. Gauthier, M. Geissel, P. Audebert, T. Cowan, M. Roth, Physical Review Letters 89 (2002) 085002.
[3] A. Macchi, M. Borghesi, M. Passoni, Reviews of Modern Physics 85 (2013) 751.
[4] J. Fuchs, P. Antici, E. d'Humières, E. Lefebvre, M. Borghesi, E. Brambrink, C. A. Cecchetti, M. Kaluza, V. Malka, M. Manclossi, S. Meyroneinc, P. Mora, J. Schreiber, T. Toncian, H. Pépin, P. Audebert, Nature Physics 2 (2006) 48.
[5] M. Passoni, L. Bertagna, A. Zani, New Journal of Physics 12 (2010) 045012.
[6] L.A. Gizzi, et al., Physical Review Special Topics – Accelerators and Beams 14 (2011) 011301.
[7] L. Labate, et al., Nuclear Instruments and Methods in Physics Research Section A 495 (2002) 148.
[8] M. Galimberti, et al., Review of Scientific Instruments 76 (2005) 053303.
[9] K. Harres, M. Schollmeier, E. Brambrink, P. Audebert, A. Blažević, K. Flippo, D. C. Gautier, M. Geißel, B.M. Hegelich, F. Nürnberg, J. Schreiber, H. Wahl, M. Roth, Review of Scientific Instruments 79 (2008) 093306.
[10] D. Jung, R. Horlein, D. Kiefer, S. Letzring, D.C. Gautier, U. Schramm, C. Hubsch, R. Ohm, B.J. Albright, J.C. Fernandez, D. Habs, B.M. Hegelich, Review of Scientific Instruments 82 (2011) 013306.
[11] J.A. Cobble, K.A. Flippo, D.T. Offermann, F.E. Lopez, J.A. Oertel, D. Mastrosimone, S.A. Letzring, N. Sinenian, Review of Scientific Instruments 82 (2011) 113504.
[12] R.F. Schneider, C.M. Luo, M.J. Rhee, Journal of Applied Physics 57 (1985) 1.
[13] G.A.P. Cirrone, G. Cuttone, M. Maggiore, L. Torrisi, F. Tudisco, Radiation Effects and Defects in Solids 165 (2010).
[14] M. Maggiore, S. Cavallaro, G.A.P. Cirrone, G. Cuttone, L. Giuffrida, F. Romano, L. Torrisi, Acta Technica CSAV 56 (2011) T266–T277.
[15] F. Schillaci, M. Maggiore, A. Velyhan, G.A.P. Cirrone, G. Cuttone, D. Margarone, G. Parasiliti Palumbo, P. Pisciotta, D. Rifuggiato, F. Romano, Journal of Instrumentation 9 (2014) T10003.
[16] C. Altana, G. Lanzalone, D. Mascali, A. Muoio, G.A.P. Cirrone, F. Schillaci, S. Tudisco, Review of Scientific Instruments 87 (2016) 02A914.
[17] S. Tudisco, C. Altana, G. Lanzalone, A. Muoio, G.A.P. Cirrone, D. Mascali, F. Schillaci, F. Brandi, G. Cristoforetti, P. Ferrara, L. Fulgentini, P. Koester, L. Labate, D. Palla, L.A. Gizzi, Review of Scientific Instruments 87 (2016) 02A909.
[18] A.G. Krygier, et al., Physics of Plasmas 22 (2015) 053102.
[19] L.A.Gizzi et al., submitted in NIMA Proceedings.